PHYSICAL REVIEW C, VOLUME 60, 051602

Multifragmentation of nonspherical nuclei

A. Le Fèvre,[1] M. Płoszajczak,[1] and V. D. Toneev[2]
[1]*Grand Accélérateur National d'Ions Lourds (GANIL), CEA/DSM–CNRS/IN2P3, Boîte Postale 5027, F-14076 Caen Cedex 05, France*
[2]*Bogoliubov Laboratory of Theoretical Physics, Joint Institute for Nuclear Research, Dubna, 141980 Moscow Region, Russia*
(Received 3 February 1999; published 6 October 1999)

Influence of the shape of thermalized source on various characteristics of the multifragmentation process, as well as its interplay with effects of the angular momentum and the collective expansion are studied for the first time and the most pertinent variables are proposed. The analysis is based on the extension of the statistical microcanonical multifragmentation model. [S0556-2813(99)50211-2]

PACS number(s): 25.70.Pq, 24.60.−k

In studying the multifragmentation process, a large range of incident energies, changing by about four orders in magnitude was covered and various types of projectiles, from protons to the heaviest available ions, were probed. The reaction mechanism is often considered in terms of a two-step scenario where the first, off-equilibrium, and dynamical step results in the formation of a thermalized source which then, in the second step, decays statistically into light particles and intermediate-mass fragments (IMF's). Assuming that the thermal equilibrium is attained, various statistical multifragmentation models were employed for the second step (see [1–3], and references quoted therein). These models were so successful in providing an understanding of basic aspects of the multifragmentation process that the deviations between their predictions and the experimental data have been often taken as an indication for dynamical effects in the multifragmentation. This kind of simplistic ''cause-effect'' interpretation may, however, be misleading due to several oversimplifying assumptions in the statistical calculations, such as, e.g., the spherical shape of the thermalized source. Indeed, one expects that the spherical shape can be perturbed during the dynamical phase and the density evolution has both compressed and rarefied zones, which can give rise to rather complicated source forms [4,5]. Perhaps more important are the angular-momentum-induced shape instabilities [6,7] which may cause large fluctuations of both the Coulomb barrier and the surface energy even for moderately high angular momenta ($L\sim 40\hbar$). Moreover, at high excitations, not only does the quadrupole stiffness become small, but also the fission saddle point moves towards larger elongations and smaller neck cross sections [7], giving rise to some ''neck effects'' [6,7]. Hence, before discussing dynamical effects in the multifragmentation decay, one should study the effects of different shapes in the freeze-out configuration. In this paper, the nonspherical fragmenting source is considered within the statistical model and the observables sensitive to the shape of this source are searched for.

Our statistical consideration is based on the microcanonical metropolis–Monte Carlo (MMMC) method of the Berlin group [1]. In the MMMC method, one calculates all accessible states equally populated in the decay of thermalized system into N fragments. The microscopic thermodynamics used here describes the dependence of the volume of $6N$-dimensional phase space on globally conserved quantities (energy, mass, charge, ...) and external constraints (such as the spatial volume) to be defined by the first stage of the reaction. Within the microcanonical ensemble method, an explicit treatment of the fragment positions in the occupied spatial volume allows for a direct extension of the MMMC code [1] to the case of nonspherical shapes. Here the source deformation is considered an additional external constraint. The main results of our paper will be given for the source described as an axial ellipsoid: $(x/R_x)^2+(y/R_y)^2+(z/R_z)^2=1$, with $R_x=R_y\neq R_z$. We assume that the freeze-out density of the deformed system is the same as that of a spherical system with the radius $R_{sys}=(R_xR_yR_z)^{1/3}$, i.e., the volume of deformed system is conserved. This condition changes neither the pass scheme nor the weight w_r due to the accessible volume of the fragments in the Metropolis scheme of calculations [1]. On the other hand, it means that the ellipsoidal source shape depends on one additional parameter: the ratio of ellipsoid axes $\mathcal{R}=R_x/R_z$. The ratio $\mathcal{R}<1$ corresponds to the prolate form, while for the oblate form one has $\mathcal{R}>1$.

An essential feature of nonspherical systems is that the deformation ''costs'' some extra energy E_{def}, which is proportional to a change of nuclear surface with respect to the spherical shape. Since we do not consider shape evolution of the system, but rather the influence of source shape on its thermodynamics, this energy E_{def} will be inaccessible for thermal motion and may be disregarded in the total energy balance. However, this point should be kept in mind if one tries to refer to the real values of energy pumped into the system.

The source deformation will noticeably affect the moment of inertia and, together with the Coulomb energy, which is calculated exactly for every multifragment configuration of nonspherical nucleus, becomes very important for describing rotating systems. As to the general scheme to account for the total angular momentum and the calculation of the statistical weight w_{pl} of the configuration in the rotating frame, we closely follow Ref. [8] to be realized in the available code.[1] For each spatial configuration of fragments, part of the total energy goes into rotation and hence the temperature of the system will slightly fluctuate. We take into account fluctuations of the moment of inertia arising from fluctuations in the

[1]In our version of the MMMC code the program error made in [8] is corrected (see also Ref. [2]).

positions of fragments and light particles. In the calculation of statistical decay of the fragmenting system, the angular velocity of the source is added to the thermal velocity of each fragment.

In calculating all accessible states within the standard MMMC method, the source should be averaged with respect to the spatial orientation of its axes, which is assumed to be homogeneously distributed in the whole 4π solid angle [1]. If the angular momentum of fragmenting system, caused by the dynamical first step of the reaction, is strictly conserved, then not all of these states will be accessible and a formal averaging over the 4π solid angle will result in the violation of angular-momentum conservation [2,8]. In the considered reactions, the angular-momentum vector is perpendicular to the reaction plane. So, we disentangle in the MMMC code the beam direction (the z axis) and the rotation axis (the x axis). The rotation energy is then $\mathbf{L}^2/2J_x \equiv L_x{}^2/2J_x$, where J_x is the rigid-body moment of inertia with respect to the x axis. Averaging over the polar angle θ is not consistent with the angular-momentum conservation. On the contrary, averaging over 2π in the angle ϕ corresponds to averaging over the azimuthal angle of the reaction impact parameter and should be included. Averaging over rotation angle ψ around $\mathbf{L}$ depends on the considered reaction, namely on the relationship between a rotation time: $\tau_{rot}=J_x/L_x$, and a characteristic lifetime of the source τ_c. For a system with high angular momentum when $\tau_{rot} \ll \tau_c$, the full averaging in $0 \leqslant \psi \leqslant 2\pi$ should be performed. In the opposite limit when $\tau_{rot} \gg \tau_c$, only states with $\psi \simeq 0$ are accessible. Below we shall consider both of these limiting cases.

In the heavy ion collisions, a part of the total energy can be stored in the compression energy of preformed source which during the collective (isenthropic) expansion is transformed into the kinetic energy of fragments. In a strict thermodynamic sense, such an expanding system is not in equilibrium. However, in the quasistatic expansion, i.e., when the time scale involved in the expansion is larger compared to the equilibration time, the system may be considered to be infinitesimally close to the thermal equilibrium and consistently treated likewise as an equilibrated system under the action of a negative external pressure whose magnitude is equal to the flow pressure. Such an approach has been applied for describing the flow effect in multifragmentation within a quantum-statistical model [9], giving an estimate of about 20 MeV/nucleon for a maximal applicable flow energy. Consistent treatment of this effect within the microscopic approach would require an introduction of proper weight factors in the MMMC code. Such a work is now in progress [10]. However, to gain some insight into the influence of collective flow on the multifragmentation process, we shall mimic this effect by simply adding the blast velocity v_b to the thermal velocity of each particle/fragment for any event simulated by the Metropolis method. This approximate procedure does not affect the Metropolis pass scheme in the original code. Assuming $\mathbf{v} \sim \mathbf{r}$, a simplified scaling solution of the nonrelativistic hydrodynamic equations describing the radial expansion of a spherical source provides the following general form for the radial velocity profile [11,12]:

$$v_b(r) = v_0 (r/R_0)^{\alpha}. \tag{1}$$

Here v_0 and R_0 are strength and scale parameters of the flow, respectively, and the power-law profile is characterized by the exponent α, which is commonly taken in the interval: $0.5 \leqslant \alpha \leqslant 2$. For the nonspherical expansion, the velocity profile may have a more complicated form and depends on the direction. But, even in the case of axially symmetric expansion, the scaling relation (1) was successfully applied for describing the profile of the transverse expansion velocity [12,13]. Below it is assumed that the radial expansion at the freeze-out point is described by Eq. (1). In the hydrodynamic interpretation, the scaling parameter R_0 corresponds to the size of the system at the initial time of the scaling regime and, therefore, it should be less than the effective radius of the spherical source at the freeze-out point, i.e., $R_0 \leqslant R_{sys}$. The strength parameter v_0 is then equal to the blast velocity at the surface of this effective sphere. As can be seen from Eq. (1), the kinetic energy of fragments produced in the ''interior'' will be mainly sensitive to the variation of the exponent α, while the total collective flow energy may be fitted by a different combination of all of these three parameters. Note that the *average* collective energy of expansion, similarly as the deformation energy, is not included in the value of the total excitation energy.

As an example, let us consider the multifragmentation of ^{197}Au having the angular momentum $L=40\hbar$ and the excitation energy 6A MeV. These parameters correspond to the source formed in central Xe+Sn collisions at 50A MeV [14]. All calculations were carried out at the standard breakup density $\rho \approx \rho_0/6$, which gives $R_{sys}=12.8$ fm for the radius of the spherical ^{197}Au nucleus. We consider two ellipsoidal shapes characterized by the axis ratio $\mathcal{R}=0.6$ (prolate shape) and $\mathcal{R}=1/0.6=1.667$ (oblate shape). We have found that none of the observables related to the fragment-size distribution is sensitive to the deformation of fragmenting source at such high excitation energies. The c.m. system angular distribution of the largest fragment, i.e., the fragment with the largest charge ($Z=Z_{max}$), is shown in Fig. 1. In the absence of collective expansion, the angular distribution is isotropic for oblate configurations and has small forward-backward peaks for prolate configurations if the averaging around $\mathbf{L}$ is performed in the whole available interval $0 \leqslant \psi \leqslant 2\pi$. For the ''frozen'' spatial configuration ($\psi=0$), the ''deformation effect'' is clearly seen; for the prolate form there are strong forward-backward peaks, while for the oblate form the heaviest fragment is predominantly emitted in the sideward direction ($\theta_{cm}=\pi/2$), as in the scenario of hydrodynamic splashing. This deformation effect is definitely not due to the angular momentum as can be seen by comparing Figs. 1(a) and 1(b) ($L=0$) with Figs. 1(c) and 1(d) ($L=40\hbar$). The collective expansion ($\alpha=2$) enhances the deformation effect. One may note a strong enhancement of forward and backward peaks in the prolate case and the appearance of a strong peak at $\theta_{cm}=\pi/2$ in the oblate case. Similar features can also be seen in the cumulative angular distributions of all IMF's, but the relative amplitude of the deformation effect in that case is smaller.

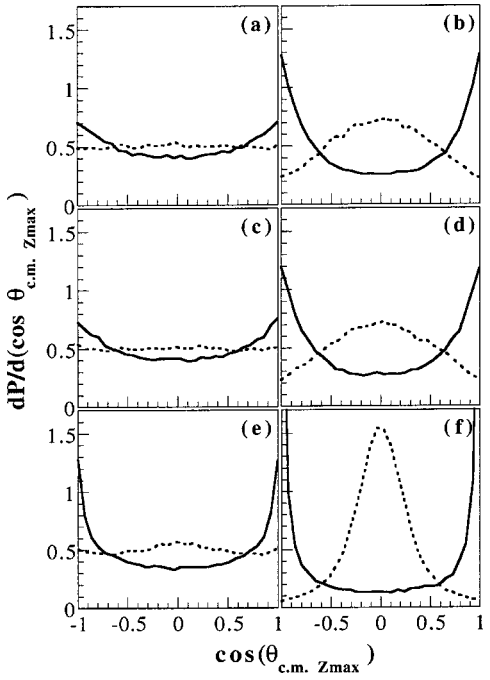

FIG. 1. Angular distribution of Z_{max} in the c.m.s. Plots on the left-hand side (lhs) correspond to averaging over the whole available interval $0 \leqslant \psi \leqslant 2\pi$, whereas plots on the right-hand side (rhs) correspond to the ''frozen'' configuration $\psi = 0$. (a) and (b), $L = 0$, $v_b = 0$; (c) and (d), $L = 40\hbar$, $v_b = 0$; (e) and (f), $L = 40\hbar$, $v_b = 0.08c$, $\alpha = 2$.

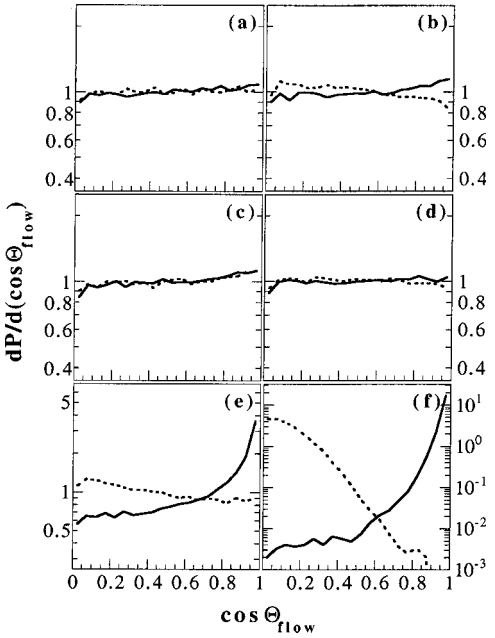

FIG. 2. Θ_{flow} distribution. The plots on the lhs correspond to the averaging over the whole available interval $0 \leqslant \psi \leqslant 2\pi$, whereas the plots on the rhs correspond to the ''frozen'' configuration $\psi = 0$. (a) and (b), $L = 0$, $v_b = 0$; (c) and (d), $L = 40\hbar$, $v_b = 0$; (e) and (f), $L = 40\hbar$, $v_b = 0.08c$, $\alpha = 2$.

Large sensitivity to the source shape is expected in the analysis using global variables on an event-by-event basis [15]. Here we shall associate the global variables with the momentum tensor:

$$Q_{ij} = \sum_{\nu=1}^{N} \gamma^{(\nu)} p_i^{(\nu)} p_j^{(\nu)}, \tag{2}$$

where $p_i^{(\nu)}$ is the ith Cartesian coordinate ($i = 1,2,3$) of the c.m.s. momentum $p^{(\nu)}$ of the fragment ν. The sum in Eq. (2) is running over all IMF's ($Z \geqslant 3$). The factor $\gamma^{(\nu)}$ depends on the physical interpretation which one wants to give to the tensor (2). We use $\gamma = 1/2m_{(\nu)}$, where $m_{(\nu)}$ is the mass of fragment ν. The tensor Q_{ij} can be represented as an ellipsoid in the momentum space. The shape of this ellipsoid can be described by three axes and its orientation can be fixed by three angles in the three-dimensional momentum space. This is usually done by referring to the eigenvalues $0 \leqslant \lambda_1 \leqslant \lambda_2 \leqslant \lambda_3$ ($\lambda_1 + \lambda_2 + \lambda_3 = 1$) of the tensor Q_{ij} and to the Euler angles defining the eigenvectors $\mathbf{e}_1, \mathbf{e}_2, \mathbf{e}_3$. From various possible combinations of these parameters defining global variables [15], we consider here the sphericity $s = (3/2)(1 - \lambda_3)$, the coplanarity $c = (\sqrt{3}/2)(\lambda_2 - \lambda_1)$, the aplanarity $a = (3/2)\lambda_1$, and the flow angle Θ_{flow} defined as an angle between $\mathbf{e}_1$ and the z direction (the beam direction) in the c.m.s.

Distribution over the flow angle is presented in Fig. 2. Different physical situations considered in Fig. 2 are exactly the same as in Fig. 1. Even though Θ_{flow} now characterizes all IMF's rather than the most sensitive largest fragment, the difference in the source shape manifests itself already for a vanishing blast velocity $v_b = 0$. The whole effect is extremely sensitive to the presence of collective expansion [see Figs. 2(e) and 2(f)] and is furthermore enhanced for the ''frozen'' configuration ($\psi = 0$). The maximal size of genuine angular-momentum effects can be seen by comparing Figs. 2(b) ($L = 0$) and 2(d) ($L = 40\hbar$). In general, one expects that the $\cos(\Theta_{flow})$ distribution for highly central events is uniform [14]. However this naive expectation may be altered by many effects, such as the spatial shape of the source, the non-vanishing collective radial expansion, the high angular momentum and, last but not least, the detection bias.

Figure 3 shows the distributions over sphericity dP/ds, coplanarity dP/dc, and aplanarity dP/da for different source deformations. By construction, these distributions do not depend on ψ averaging. The curves plotted with bold lines correspond to nonvanishing collective expansion, which reveals different ellipsoidal source shapes. The reason for this sensitivity can be seen from Eq. (1). Depending on the source shape, a different number of fragments can be placed in the two regions $r < R_0$ and $r > R_0$ (we put $R_0 = 0.7R_{sys}$ everywhere), in which the expansion acts differently. For the same reason, these distributions are insensitive to the radial expansion for the spherical source. Particularly interesting are the sphericity and coplanarity distributions where the evolution of distributions with v_b is clearly different for prolate and oblate source shapes. The lack of sensitivity of the aplanarity distribution to the deformation effects and to the expansion happens accidentally for chosen parameters. One should also mention that the sensitivity of dP/ds and dP/dc distributions to the source deformation and their

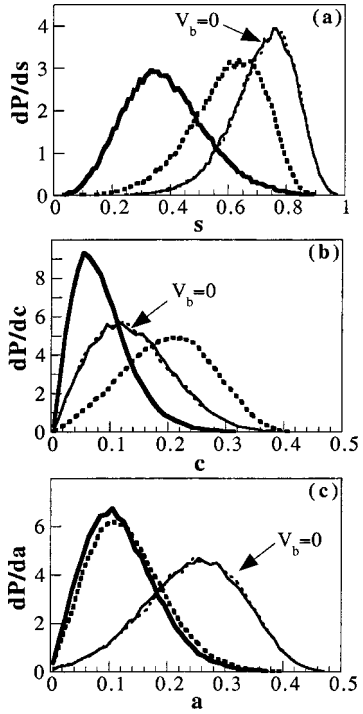

FIG. 3. (a) Sphericity, (b) coplanarity, and (c) aplanarity distributions for $L=40\hbar$. Bold lines correspond to $v_b=0.08c$, $\alpha=2$. The continuous lines show the prolate $\mathcal{R}=0.6$ shape, whereas dashed lines show the oblate $\mathcal{R}=1.667$ shape.

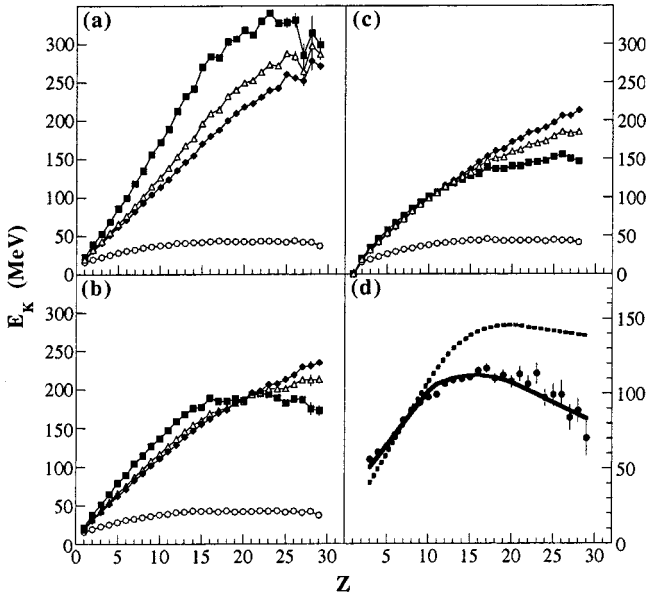

FIG. 4. Kinetic energy of fragments is plotted as a function of Z. (a) Prolate shape, $L=40\hbar$. Different curves correspond to $v_b=0$ (circles) $v_b=0.08c$, $\alpha=1/2$ (diamonds), 1 (triangles), and 2 (squares). (b) The same as in (a) but for the oblate shape. (c) The same as in (a) but for the spherical shape. (d) The comparison between the experimental data and the calculation ($\alpha=2$) for both prolate and oblate freeze-out configurations and the blast velocities: $v_b=0.088c$ (prolate shape), $v_b=0.063c$ (oblate shape), chosen to reproduce the experimental mean kinetic energy per nucleon of IMF's : 5.2 ± 0.1 MeV/nucleon.

insensitivity to the time scales involved (the ψ averaging) provides interesting and supplementary information to those contained in the Z_{max} angular distribution and in the $\cos(\Theta_{flow})$ distribution.

The Z dependence of average kinetic energy E_k of IMF's for diffferent source shapes and different α parameters is shown in Fig. 4. The calculations have been done for the ''frozen'' configuration ($\psi=0$). The collective expansion energy is a dominant contribution to the average kinetic energy of fragments, and its value differs noticeably for prolate and oblate source shapes. It is of interest to note that the average kinetic energy of fragments exhibits a flattening or even a maximum at large Z (see, e.g., the curve for $\alpha=2$). The precise position of this maximum also depends on the deformation [see Figs. 4(a) and 4(b)]. An attempt to reduce this large observed kinetic energy to angular-momentum effects results in a value of the average angular momentum ($L\approx640\hbar$) which is completely unrealistic for selected central events [14]. Figure 4(c) shows $E_k(Z)$ for the spherical source shape. Figure 4(d) compares results of the present model with the experimental data for central Xe+Sn collisions at 50A MeV [14]. All calculated events have been filtered with the INDRA software replica, and then selected with the experimental centrality condition: complete events (i.e., more than 80% of the total charge and momentum is detected) and $\Theta_{flow}\geqslant\pi/3$.

In conclusion, external constraints on the shape of the equilibrized fragmenting source have been considered within the extended MMMC method. Due to the change in the Coulomb energy for deformed freeze-out configuration, the shape effect is clearly seen in the IMF's angular distributions (Z_{max} angular distribution) as well as in the Θ_{flow} distribution. A surprising interplay between effects of nonspherical freeze-out shapes and the memory effects of nonequilibrium phase of the reaction, such as the rotation and the collective expansion of the source, has been demonstrated for the first time. The influence of shape on rotational properties of the system is not only reduced to the modification of the momenta of inertia. The limits on the averaging interval over the angle ψ about the rotation axis, which are defined by the appropriate time scales, strongly affect the angular observables and are able to strongly enhance the ''shape effect.'' These constraints may be important for certain observables used in experimental procedures of selecting specific class of events. Another striking finding is that the collective expansion allows disclosure of the source shape in the analysis using global variables, as well as in the study of the Z dependence of the average kinetic energy. The latter observable is independent of ψ averaging but, unfortunately, it is specified by a poorly known profile function (1). Nevertheless, the careful analysis with Eq. (1) might shed some light on the problem of how different fragments are situated in the freeze-out configuration.

In the experimental analysis, if the average kinetic energy of fragments is fixed by an appropriate choice of v_b, R_0 for each source deformation, then the shape of $E_k(Z)$ contains information about the exponent α in the parametrization (1) and, to the lesser extent, about the deformation of the source.

The form of the dP/ds and dP/dc distributions then permits one to find the average deformation of the fragmenting source. Having fixed the parametrization (1) and the deformation of the source, the analysis of the angular distribution of Z_{max} and/or the Θ_{flow} distribution gives access to the information about the time constraints (the limits on the ψ averaging) in the multifragmentation process. We have discussed here the freeze-out shape effect for only one value of the excitation energy. Certainly, the manifestation of this effect in observables is energy/angular-momentum dependent and the modifications of the MMMC method, presented in this Rapid Communication, open a promising way to follow up the shape evolution of equilibrized source in the broad range of incident energies. Alongside of the observables discussed here, it would be interesting to study the velocity correlations between fragments that are sensitive to the source shape at the freeze out. Such work is now in progress [10].

We are grateful to D.H.E. Gross for his encouragement and interest in this project. We are thankful to O. Shapiro for the implementation of the original version of the MMMC code. We also thank G. Auger, A. Chbihi, and J.-P. Wieleczko for their interest in this work. This work has been supported by the CNRS-JINR Dubna Agreement No. 98-28.

[1] D.H.E. Gross, Rep. Prog. Phys. **53**, 605 (1990).
[2] D.H.E. Gross, Phys. Rep. **279**, 119 (1997).
[3] J.P. Bondorf, A.S. Botvina, A.S. Iljinov, I.N. Mishustin, and K. Sneppen, Phys. Rep. **257**, 133 (1996).
[4] K.K. Gudima, H. Iwe, and V.D. Toneev, J. Phys. G **5**, 229 (1976).
[5] W. Bauer, G.F. Bertsch, and H. Schulz, Phys. Rev. Lett. **69**, 1888 (1992); L.G. Moretto, Kin Tsuo, N. Colonna, and G.J. Wozniak, *ibid.* **69**, 1884 (1992); B. Borderie, B. Remaud, M.F. Rivet, and F. Sebille, Phys. Lett. B **302**, 15 (1993).
[6] S. Cohen and W.J. Swiatecki, Ann. Phys. (N.Y.) **82**, 557 (1974).
[7] M.E. Faber, M. Płoszajczak, and K. Junker, Acta Phys. Pol. B **15**, 949 (1984).
[8] A.S. Botvina and D.H.E. Gross, Nucl. Phys. **A592**, 257 (1995).
[9] S. Pal, S.K. Samaddar, and J.N. De, Nucl. Phys. **A608**, 49 (1996).
[10] A. Le Fèvre, M. Płoszajczak, and V.D. Toneev (unpublished).
[11] J.P. Bondorf, S.I.A. Garpman, and J. Zimányi, Nucl. Phys. **A296**, 320 (1978).
[12] T. Csörgo, B. Lörstad, and J. Zimányi, Phys. Lett. B **338**, 134 (1994).
[13] A. Polleri, J.P. Bondorf, and I.N. Mishustin, Phys. Lett. B **419**, 19 (1998).
[14] R. Bougault *et al.* (INDRA Collaboration), *Proceedings of the XXXV International Winter Meeting on Nuclear Physics*, Bormio, 1997, edited by I. Iori (Università degli Studi di Milano, Supplemento 103, 1997), p. 251; N. Marie *et al.* (INDRA Collaboration), Phys. Lett. B **391**, 15 (1997); A. Le Fèvre, Ph.D. thesis GANIL T 97 03; S. Salou, Ph.D. thesis GANIL T 97 06.
[15] J. Cugnon and D. L'Hôte, Nucl. Phys. **A397**, 519 (1983).